Title
Multiparticle Production in p-Nucleus and Nucleus-Nucleus Collisions

Authors
Hoang, T.F.
Crawford, H.J.

Publication Date
1989-09-01

UC-413
LBL-27799
Preprint

Lawrence Berkeley Laboratory
UNIVERSITY OF CALIFORNIA

To be submitted for publication

Multiparticle Production in p-Nucleus and Nucleus-Nucleus Collisions

T.F. Hoang and H.J. Crawford

September 1989

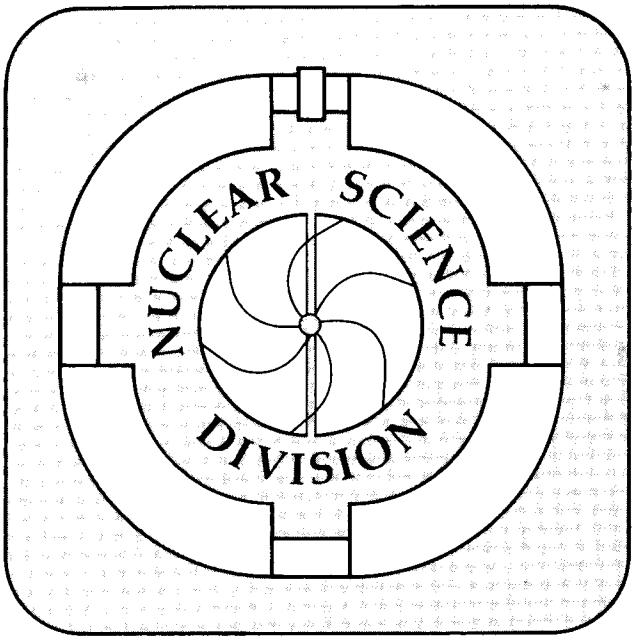

Prepared for the U.S. Department of Energy under Contract Number DE-AC03-76SF00098.

DISCLAIMER

Multiparticle Production in p-Nucleus and Nucleus-Nucleus Collisions*

T.F. Hoang
1749 Oxford Street
Berkeley, California 94709

and

H.J. Crawford
Space Sciences Laboratory
Lawrence Berkeley Laboratory
Berkeley, California 94720

Kinematic properties of inclusive $p + A \rightarrow \pi^-$ and $A_1 + A_2 \rightarrow \pi^-$ at 200 GeV/nucleon are compared with $p + p \rightarrow \pi^-$ at 200 GeV/c using data of CERN-SPS experiments. The partition-temperature is found to be practically the same for all the reactions analyzed, suggesting an approximate scaling. The peak shift of pseudo-rapidity η distributions of these nuclear reactions with respect to the peak of $pp \rightarrow \pi^-$ follows a geometrical law: $\eta^* \simeq (A_2^{1/3} - A_1^{1/3})/8$, independent of energy. The mfp ℓ characteristic of the energy loss suffered by the projectile fireball passing through the nuclear target is $\ell \simeq 6.21$ fm. Semi-empirical formulae for $<n_->$ of $p + A$ and $A_1 + A_2$ reactions are proposed and tested using available data.

*This work was supported by the Director, Office of Energy Research, Division of Nuclear Physics, Office of High Energy and Nuclear Physics, of the U.S. Department of Energy under Contract No. DE-AC03-76SF00098, and by NASA under Grant NGR05-003-513.

1. Introduction

Ever since the discovery of large stars in emulsion produced by heavy nuclei of the primary cosmic rays,[1] forty years ago, great interest has been paid to the study of these high-energy nucleus-nucleus reactions. It is a challenge to understand this problem of fundamental importance: How is the pre-matter created?[2] Recently, experiments of high-energy heavy-ion (HI) reactions at the CERN-SPS and BNL AGS-Tandem[3] indicate an abundance of mesons produced in the central region where a phase transition to a quark-gluon plasma is expected to occur according to QCD prediction.[4]

The salient feature of these nuclear reactions is the average $P_\perp$ of secondaries from various targets, which is practically the same for the same energy per incident nucleon, see Tables I and II. This suggests that the primary interaction proceeds like pp, namely collision of an incident nucleon with a free nucleon inside the nucleus, followed by secondary collisions with other nucleons of the target.

An attempt is therefore made to analyze the pseudo-rapidity η distributions of $p + A \rightarrow \pi^-$ and $^{16}O + A \rightarrow \pi^\pm$ at 200 GeV/nucleon of CERN-SPS experiments[5–7] as in the case of $\pi^+ p$ and $K^+ p \rightarrow \pi^-$ of a previous work[9b] using the Chou-Yang-Yen (CYY) formula,[8] generalized by introducing the shift parameter η^* to account for the asymmetry of the distribution with respect to the axis $\eta = 0$ in the cms of the colliding nucleons, Figs. 1 and 2 (Sec. 2).

The results of our analysis unravel interesting properties of a geometrical aspect of multiparticle production by high energy p+A and HI reactions (Secs. 3 and 4), especially the behavior of the shift parameter $\eta^* \sim A^{1/3}$ (Sec. 5) and the approximate scaling of the η-distribution, Fig. 4, as is expected from the generalized CYY formula (5) (Sec. 6).

The energy loss of the forward FB of $p + A \rightarrow \pi^- + \cdots$ passing through the target nucleus of mass number A is investigated using the data of x-distributions of a MIT-Fermilab experiment at 100 GeV/c.[11] We find a mfp $\simeq$ 6.2 fm comparable to the U radius (Sec. 7). The energy dissipated in the target nucleus serves to create secondary mesons emitted by the target.

We find practically the same T_p^* (in the FB system) for p+ nucleus and ^{16}O+ nucleus collisions as for pp at the same GeV/nucleon, Tables I and II, indicating that in the central region, the energy-density is the same for the reactions we have analyzed and that the primary act of interaction is like a nucleon-nucleon collision followed by secondary interactions in the nuclear target. This mechanism leads to a semi-empirical formula for the ratio of negative multiplicities of pA to pp, Eq. (16), in good agreement with experimental values from $P_{lab} = 9.9$ to 360 GeV/c (Sec. 8). The formula is extended to the HI reactions, Eq. (18) and charged multiplicity, Eq. (19).

Some remarks will be made (Sec. 10) on the geometrical properties of multiparticle production by nuclear reactions, especially the application of Chou-Yang-Yen formula, Eq. (5) which enables us to get insight into this complex problem of high energy HI reactions.

2. The partition-temperature Model

In an attempt to investigate the kinematic properties of multiparticle production by high energy nuclear reactions of CERN-SPS experiments (see below) we are led to analyze the pseudorapidity $\eta = -\ln(\tan \theta/2)$ distributions (Figs. 1 and 2) in the context of the partition-temperature T_p model of Chou, Yang and Yen (CYY).[8] Consider first the case of inclusive

$$p + p \rightarrow \pi^- + \cdots \quad ,$$

as has been reported previously,[9a] we may use the CYY formula for the η distribution of zero mass particles in the cms of collision

$$\frac{dn}{d\eta} = \frac{N}{(\alpha + \frac{1}{T_p}\cosh\eta)^2} \tag{1}$$

where $\alpha = 2/\langle P_\perp \rangle$ is a fixed parameter corresponding to a cut-off on the transverse momentum, T_p the partition temperature, and N the normalization coefficient.

Note that in the case of fixed-target experiments, the passage from the lab system to the cms is straightforward:

$$\eta_{lab} = \eta + \eta_{cm} \tag{2}$$

where $\eta = \ln (\cot \theta_{cm}/2)/$ is the pseudo-rapidity of a secondary in the cms of colliding pp and η_{cm} is that of the pp cms with respect to this lab system, namely

$$\eta_{cm} = \frac{1}{2} \ln \frac{1 + \beta_{cm}}{1 - \beta_{cm}} \simeq \frac{1}{2} \ln \frac{2P_{lab}}{m_p} \tag{3}$$

β_{cm} being the velocity of the pp cms in the lab system.

We recall that T_p in (1) represent the average energy of produced secondaries in their *rest-frame* referred to as the *initial* fireball (FB), which subsequently splits into two: one forward (FD) and another backward (BD), associated to the colliding protons. Clearly, these two FB's are symmetric just as the system pp in the initial state, so that their cms coincides with the cms of the colliding pp.

As regards $p + A \rightarrow \pi^-$, there are more π's in the BD direction than in the forward, as is seen from Fig. 1. Note that the asymmetry is still more striking in the case of HI

reactions $^{16}O + A$ as is shown in Fig. 2.

Therefore, to apply the CYY formula (1), to the asymmetric η-distributions we are dealing with, we have to use an appropriate frame, namely the *initial* FB rest-frame before its break-up into FD and BD associated to the projectile and the target nucleus, disregarding the cms of the primary collision of the incident nucleon with a nucleon of the target-nucleus, and that because of other π's from secondary reactions inside the target nucleus. For this purpose, we replace in (1)

$$\eta \rightarrow \eta - \eta^* \tag{4}$$

and write

$$\frac{dn}{d\eta} = \frac{N}{(\alpha + \frac{1}{T_p^*}\cosh(\eta - \eta^*))^2} \tag{5}$$

where the asterisk is to specify the rest-frame of the *initial* FB in which the partition temperature should be estimated. Note that α is invariant like $<P_\perp>$ (see above). Now, if η^*_{FB} and η^*_{BD} (<0) are rapidities of the FD and BD fireballs (see below),

$$\eta^* = \eta^*_{FD} + \eta^*_{BD} \quad . \tag{6}$$

which relates T_p^* to T in (1) as has been discussed in Ref. 9(b). Note that $\eta^* = 0$, if $\eta^*_{FD} = |\eta^*_{BD}|$, i.e. the FD and the BD FB's are symmetric.

As regards the kinematics of the FB, we note that its velocity β^* may be estimated by using the covariant Boltzmann factor as follows

$$f \approx e^{-(E-\beta^* P_{||})/T} \tag{7}$$

where $(E, \vec{P})$ are the energy and the momentum in cms of a secondary particle of p + A

$\rightarrow \pi^-$, in one hemisphere and T the conventional temperature determined by $<P_\perp>$ (see, e.g., Ref. 4). As reported previously,[11] β^* may be estimated independently of T by using the cms angular distribution; or else we use the distribution of $x = 2P_{||}/\sqrt{s}$, namely

$$\frac{dn}{dx} \sim x\, e^{-ax} \tag{8}$$

according to (7), with

$$a \equiv (1 - \beta^*)\sqrt{s}/2T \quad . \tag{9}$$

Finally, we mention that the Boltzmann factor (7) resembles that used by Fermi for the angular momentum conservation of secondary particles,[12] whereas Li and Young use the factor (7) for their partition-temperature model of p-nucleus reactions[13] regarding β^* as the FB velocity.

3. Inclusive $p + A \rightarrow \pi^-$ reactions

We now proceed to analyze the data of $p + A \rightarrow \pi^-$ at 200 GeV/c of the NA5 Collaboration,[5] and NA35 Collaboration.[6] Their measurements of $<n_->$ and $<P_\perp>$ (in MeV/c) are summarized in Table I. It is interesting to note that $<P_\perp>$ is practically the same for $p + A \rightarrow \pi^-$ as for $p + p \rightarrow \pi^-$, suggesting that the primary interaction of p-nucleus reaction takes place with a single nucleon of the target, the Fermi motion being negligible.

With this assumption, we find from (3) $\eta_{cm} = 3.03$. The η-distributions in the cms of the incident p and a nucleon of the target A are shown in Fig. 1. The asymmetry is conspicuous by referring to the line at $\eta = 0$, namely the F/B ratio of π^- is < 1: compared to 1.04 ± 0.02 for $p+p \rightarrow \pi^-$ of the same experiment, which is symmetric, according to parity conservation of strong interactions.

As we do not have the x-distributions of these reactions, we are unable to determine η^* using (6). We therefore use the CYY formula (5) to fit the data leaving both η^* and T_p^* as free-parameters, whereas α is computed using the values of $\langle P_\perp \rangle$ Table I. The estimates of T_p^* (GeV) and η^* thus obtained are listed in Table I.

Note that for $p + p \rightarrow \pi^-$, $\eta^* = 0.022 \pm 0.006$ consistent with zero as should be for symmetric distributions. We therefore set it equal to zero. The shifts η^* for pA r and pXe are shown by the dot-dash segments in Fig. 1.

A comparison with the data indicates that the fits are satisfactory, especially in the region around the peak. Here, we find the sea-gull effect attenuated, in contrast to the case of $h^+p \rightarrow \pi^-$ of a previous work.[9a] This justifies a posteriori the assumption of a constant $\alpha = 2/\langle P_\perp \rangle$.

The partition-temperatures of p-nucleus reactions are comparable to that of pp, within large errors, as in the case of T determined by $\langle P_\perp \rangle$ as is listed in Table 1 (see footnote 21). For the parameter η^* which describes the asymmetry of the FB's associated to projectile proton and the target nucleus, Eq. (6), it increases with the size of the target, its A-dependence will be investigated later on, together with the nucleus-nucleus reactions (Sec. 6).

Finally, it is to be noted that we have also analyzed the η-distribution of *charged secondaries* of p + Xe. We find $\eta^* = 0.52 \pm 0.03$ and $T_p^* = 0.911 \pm 0.085$ GeV, indicating the same shift in the peak of the distribution, whereas T_p^* is somewhat greater than that of $p + X_e \rightarrow \pi^-$, as is listed in Table I. This difference may be caused by the mixture of nuclear particles of the target evaporation (see Sec. 9).

4. HI reactions $^{16}O + A \rightarrow h^{\pm}$

Turn next to the CERN-SPS experiments $^{16}O + A$ at 200 GeV/nucleon of the WA80 collaboration.[7] As is well known, the multiplicities of these high energy HI reactions are extremely high, the ratios of $<n_->$ for HI reaction to p-nucleus of the same A at P_{lab} = 200 GeV/c are listed in Table IIIb. But, in spite of the large number of secondaries emitted in these HI reactions, the average transverse momentum of ~350 MeV/c remains almost the same as $<P_\perp>$ of p-nucleus and pp reactions at P_{lab} = 200 GeV/c (see Table I). This indicates that the secondaries observed in the final state of a HI reaction result from a *superposition* of primary interactions, each of which is a nucleon-nucleon collisions, one from the projectile and another from the target, their Fermi motions being negligible.

We are therefore led to analyze the η -distributions of the WA80 collaboration[7a] (in lab system), reproduced in Fig. 2, error bars being hidden by the data points. For convenience, as in the previous case of p + A, we set η_{cm} = 3.03 and α = 5.41. The parameters thus obtained are summarized in Table II. The fits are shown in Fig. 2. They are very satisfactory, indeed. Here again, we find little sea-gull effect as in the case of inclusive p + A reactions discussed in the preceding section.

We find T_p^* comparable to those of p + A and pp as is expected from the fact that the temperature for these heavy-ion reactions, T ~ 142 MeV, corresponding to $<P_\perp> \simeq$ 350 MeV/c is comparable to those of p + A and pp listed in Table I. Therefore, the average energy density in the central region is about the same for all nuclear reactions, p + A and $A_1 + A_2$ alike, as for pp at the same incident energy/nucleon.

Consider next the parameter η^* in Table II. We note that η^* increases monotonically with the nuclear size A of the target, Fig. 3, indicating that the maximum of the η-

distribution, according to (6), shifts backward or forward according to the relative size of the target compared to the projectile. Note especially that η^* of the C target is negative.

Finally, it should be mentioned that the backward shift of maximum has been reported by the authors of the WA80 collaboration[7] and reported that "new phenomenon can not be excluded." It is therefore expedient to investigate the properties of this parameter η^* we have used to generalize the CYY formula (1) to account for the asymmetry of FB's associated with the projectile and the target.

5. The A-dependence of η^*

As has been mentioned above (Secs. 1 and 2), the shift η^* of the maximum of the η-distribution is essentially a kinematic effect. It reflects the asymmetry of the FB's associated with the projectile A_1 and the target A_2, just as in the case of inclusive $\pi^+p \to \pi^-$ or $K^+p \to \pi^-$ discussed elsewhere.[9b] Since the FB's move along the collision axis, in the opposite direction, we expect the effect of η^* to be a function of the linear dimensions of the projectile A_1 and the target A_2.

Indeed, the $A_2^{1/3}$ dependence of η^* is self-evident from the point of view the effective E_{lab} of the projectile which decreases as it passes inside the nucleus (see Sec. 7). This is shown by the plot of η^* values of p + A and ^{16}O + A listed in Tables I and II. Remembering that $\eta^* = 0$ for symmetric FB's, i.e., collision of like particles, $A_1 = A_2$, we therefore write

$$\eta^* = c(A_1^{1/3} - A_2^{1/3}) \tag{10}$$

and find by the least-squares fit for p + A and ^{16}O + A analyzed in Secs. 3 and 4; the pp case being included as a constraint of the fit:

$$-c = 0.127 \pm 0.020 \quad .$$

The fit is good, except for the deviation of the p + Ar point. This may well be due to statistics: i.e., the NA5 experiment disposes of 2000 pictures for pAr amounting to 1/2 of pXe pictures which have larger cross-section.

Next, an attempt is made to investigate the energy dependence of η^*. For this purpose, we tentatively make use of the *preliminary* data of BNL experiment E802 ^{28}Si + A at 14.5 GeV/nucleon using Al, Cu, Ag and Au targets.[14] The η^*'s are shown in Fig. 3 by crosses, they fall perfectly on the fitted straight line for the CERN-SPS experiments; to the point that if we do the same fit for the BNL points only, we then get

$$-c = 0.128 \pm 0.007$$

in excellent accord with the previous fit for the CERN-SPS data.

It is worth noting that the size of the ^{27}Al target is very close to the ^{28}Si target. We find from their data $\eta^* = 0.04 \pm 0.02$ consistent with zero, suggesting that η^* changes sign according to the relative size of the target and the target.

This remarkable property of geometrical aspect of the η^* parameter is a characteristic feature of particle production in the central region of nuclear reactions. The authors of WA 80 find all *backward* (in their notation) shifts of maximum, independent of the mass number of the target.

6. Scaling of the η-distribution

We continue to investigate the behavior of T_p^* of HI reactions in Table II. Apart from the case of Cu, the values of T_p^* for C, Ag and Au are practically the same within large statistical errors[21] and $I/T_p^* < \alpha$ which is the same for all the reactions under

consideration as $\langle P_\perp \rangle$.

Consequently, the η-distributions in Fig. 2 may be superimposed into one pattern, if we slide each distribution by $-\eta^*$ and divide it by the normalization coefficient of (5), as is expected from the generalized CYY formula (5).

Figure 4 shows the plots of $1/N_\sigma \cdot dn/d\eta$, i.e. percentage of secondaries vs. $\eta_{lab} = \eta + 3.03$ of ^{16}O + A of the WA80 Collaboration.[7] We see the scaling property for Cu, Ag and Au, whereas the carbon data deviates systematically from this property, especially in the target region. We shall leave aside the C data in the following analysis.

If we try an overall fit to the Cu, Ag and Au data in Fig. 4 using the CYY formula and assuming the same $\alpha = 5.41$ as before (Sec. 4), we find

$$\overline{T_p^*} = 0.93 \pm 0.04 \text{ GeV} \ .$$

The fit is shown by the solid curve in Fig. 4, in satisfactory agreement with the data of Cu, Ag and Au.

It should be mentioned that the partition temperature $\overline{T}_p^*$ thus obtained is significantly higher than the estimates of T_p^* of individual fits in Table II, indicating that the scaling we are dealing with is only approximate.

Finally it should be mentioned that the scaling here discussed is different from that of Nakamura and Kudo.[22] Their approach is based on the well-known KNO scaling for the multiplication of inclusive reactions, namely they plot against $\eta/\langle\eta\rangle$.

7. Passage of the projectile FB through a nuclear target

When the projectile FB of $p + A \rightarrow \pi^-$ passes through the target A, it interacts with the nuclear stuff, i.e., nucleons, mesons, etc., so it slows down and loses energy. The energy thus dissipated is used for secondary production inside the target. We therefore have to compute the velocity β^* of the projectile FB (in the cms of collision), or its Lorentz factor $\gamma_F = 1/\sqrt{1 - \beta^{x2}}$.

We recall that the FB at the initial stage of the reaction is that of $p + p \rightarrow \pi^-$ at the same energy $\sqrt{s}$ and that β^* is given by the scaling property discussed previously,[11] namely $\beta^* = 1 - 2/\gamma_{cm}$ with $\gamma_{cm} = \sqrt{s}/2m_p$.

After its passage through the nuclear target, we have to estimate β^* using the forward x-distribution of $p + A \rightarrow \pi^-$ at the formulae (8) and (9) to compute γ_F. As we do not have the x-distributions of the CERN-SPS experiments we are dealing with in the present work, we will use the data of a Fermilab experiment E116, $p + A \rightarrow \pi^-$ at 100 GeV/c of the MIT-Fermilab collaboration,[15] with p, C, Cu and Pb targets. We analyze their data of $Ed\sigma/dp^*$ at $P_\perp = 0.3$ GeV/c, using (8) and assuming T = 139 MeV to estimate β^* and γ_F. The results thus obtained are plotted in Fig. 4 vs. the specific effective radius R/r where $R = \sqrt{\sigma_{ine}/\pi}$ and r is the nuclear radius parameter.

We recall that according to the optical model:[16a]

$$R(A) = r(A^{1/3} - \frac{a}{A^{1/3}}) \tag{11}$$

account being taken of the absorption by the second term:

$$a = (\lambda/2r)^2 \tag{12}$$

λ being the absorption mfp. From a previous analysis of pA reactions at P_{lab} = 10 to 100 GeV/c, we get for the parameters (in fm)[16]

$$r = 1.30 \pm 0.01 \quad , \quad \lambda = 1.44 \pm 0.23 \quad .$$

It is worth noting that $\lambda \simeq 1/m_\pi$.

If we describe the behavior of γ_F of the projectile FB by an exponential law with a characteristic mfp ℓ , namely

$$\gamma_F \sim \exp(-R/\ell\,\gamma_{cm}) \tag{13}$$

which $\gamma_{cm} = 7.37$ is the Lorentz contraction factor. We find

$$\ell = 6.21 \pm 0.03 \text{ fm} \quad .$$

The fit shown by the curve in Fig. 5 is satisfactory.

It is interesting to note that this mfp is quite comparable to the U radius; but somewhat between 4.9 and 8 ± 2 fm estimated by Csernai, et al.[17a] and by S. Date, et al.[17b] for the mean degradation-length of the proton of inclusive p + A → p +... at 100 GeV/c of the same MIT-Fermilab experiment,[15] as analyzed here.

8. The multiplicity

As is well known, the property of limiting fragmentation holds for p + A → π^- as is reported by the MIT-Fermilab experiment.[15] Therefore, we may separate its multiplicity into forward (FD) and backward (BD) parts corresponding to the fragmentations of the projectile p and the target nucleus A, respectively:

$$\langle n- \rangle_{pA} = \langle n- \rangle_p + \langle n- \rangle_A \tag{14}$$

with

$$\langle n- \rangle_p = \frac{1}{2} \langle n- \rangle_{pp} \tag{15}$$

at the same energy, which can be predicted accurately using the scaling property of inclusive $p + p \rightarrow \pi^-$.[16b]

As regards $\langle n_- \rangle_A$, in addition to the mesons produced in the primary interaction of one of its constituent nucleons with the incident p, there are also secondary mesons arising from the energy-loss of the projectile FB and rescattering of particles inside the target nucleus. We may, for simplicity, describe these secondary processes in terms of an empirical power law: A^α, which is, to some extent, equivalent to the Glauber theory.[18] Therefore, we propose to describe the A dependence of $\langle n_- \rangle_{pA}$ by a semi-empirical formula as follows, in form of a ratio to $\langle n_- \rangle_{pp}$ at the same energy:

$$R(A) = \langle n_- \rangle_{pA} / \langle n_- \rangle_{pp} = \frac{1}{2} (1 + A^{\alpha/3}) \tag{16}$$

where we have expressed explictly the target dimension, $A^{1/3}$, a property of geometric aspect discussed above. The parameter α to be estimated using the experimental data is expected to be ~1. Note that (16) may be derived from the multiple collision model by keeping only the leading term corresponding to one collision.

We use the negative multiplicity from $p + A \rightarrow \pi^- + ...$ at 200 GeV/c listed in Table I to estimate the parameter α; with the pp case serving as a constraint, namely $R(1) \equiv 1$. We get

$$\alpha = 0.80 \pm 0.16$$

The predicted multiplicities, Table IIIa, agree rather well with the experimental ratios.

As a consistency check of our parametrization, we have used other available data of $p + A \rightarrow \pi^-$, with different targets and at different energies, from $P_{lab} = 9.9$ to 360 GeV/c.[19] The predictions by (16) are in Table IIIa. The agreement is satisfactory, indicating that α is likely not sensitive to the energy and that $\alpha \neq 1$ by ~ one sd is probably due to some screening effect in the rescattering process.

As regards the multiplicities of HI reactions, we may extend (16) for $p + A \rightarrow \pi^-$ to nucleus-nucleus reactions: $A_1 + A_2 \rightarrow \pi^-$. We make use of this property of their cross-sections according to the optical model, reported previously:[16a]

$$A^{1/3} \rightarrow A_1^{1/3} + A_2^{1/3} \tag{17}$$

and assume the large A approximation to get, as in the case of (16),

$$R\,(A_1,A_2) = \langle n_- \rangle_{A_1A_2} / \langle n_- \rangle_{pA_2} = C[1 + (A_1^{1/3} + A_2^{1/3})^{\beta}] \tag{18}$$

where β is a parameter to be compared with α of (16) and C a coefficient such that $R(1,1) = 1$ as a consisteny check (see below).

We use the data of a streamer chamber experiment $^{16}O + A \rightarrow \pi^- + \cdots$ at 200 GeV/A by the NA35 collabration.[6] The experimental ratios $R(A_1,A_2)$ are listed in Table IIIb, the values of $\langle n_- \rangle_{pA_2}$ being computed by (16). Note that the effective mass number of the mixture 20% He and 80% Ne is 15.7 close to that of the oxygen projectile; we find

$$\beta = 1.91 \pm 0.18$$

$$C = 0.26 \pm 0.02$$

The computed ratios are listed in Table IIIb, in excellent agreement with the experimental values. As a consistency check of our parametrization, we have computed the ratio

(18) for $A_1 = A_2 = 1$ and found $R(1,1) = 1.24 \pm 0.26$ consistent with $R(1,1) = 1$ according to the definition (18). Next, we note that $C = 0.26$ is about 1/2 of the corresponding coefficient in (16) for $p + A \rightarrow \pi^-$. This is expected from the symmetry of $R_{12}/r = A_1^{1/3} + A_2^{1/3}$, more specifically, (18) remains the same for the reversed reaction $A_1 \overrightarrow{\leftarrow} A_2$. The HI reactions we are dealing with are fixed target experiments, the reversed reactions being unaccounted for. In this regard, we have to bear in mind that the cms energy $\sqrt{s}$ may be different for the reversed reaction so that the direct and the reversed HI reactions may not be treated on the equal footing.

As regards the charged multiplicity, we find that it may be expressed in terms of $<n_->$ by means of the charges Z_1 and Z_2 of the projectile and the target as follows:

$$<n_{ch}> = <n_-> \frac{A_1 + A_2}{Z_1 + Z_2} \quad . \tag{19}$$

Note that (19) holds also for the p-nucleus reactions of NA-35 collaboration[6] discussed above.

Finally, we note that

$$\beta \simeq 2\alpha \tag{20}$$

suggesting that the pion production by HI reactions is rather a surface emission than a bremsstrahlung around the collision axis as in the case of $p + A \rightarrow \pi^-$ with $\alpha \simeq 1$ as expected from Landau's model.

10. Concluding remarks

The results of our analysis of the η-distributions of p-nucleus and HI reactions of CERN-SPS experiments at the same energy 200 GeV/nucleon[5-7] using the formula (5) of

the partition-temperature T_p model of Chou, Yang and Yen[8] indicate that T_p^* in the FB system is practically the same as for the $p + p \rightarrow \pi^-$ at $P_{lab} = 200$ GeV/c. The fits, Figs. 1 and 2, are excellent, especially for the HI reactions, compared to the fits presented by the authors of the NA80 collaboration using the Fritiof model.[7a]

We have introduced the shift η^*, Eq. (4), to describe the asymmetry of the FB's in nuclear reactions, in analogy with $\pi^+p \rightarrow \pi^-$ compared to $pp \rightarrow \pi^-$ reported previously.[9b] This parameter describes the *peak-shift* of η-distributions observed by the WA80 collaboration, but "not understood."[6a] We find that η^* has this simple and remarkable property of geometrical aspect, namely $\eta^* \sim A^{1/3}$ and independent of energy Fig. 3. However, no such peak-shift has been observed in emulsion data.[20] This may be due to the systematics of using the shower tracks with $\beta > 0.7$ and the mixture of nuclear particles from Br and Ag targets. It is not known how these causes may affect the shape of the η-distribution near the maximum.

The salient feature of the η-distributions of p-nucleus and HI reactions, Figs. 1 and 2, analyzed in the present work is that T_p^* is practically constant within large errors. Consequently, according to the generalized CYY formula (5), the η-distributions have the scaling property (Sec. 6). However, we find it valid only for HI reactions of large target, at variance with the scaling proposed by Nakamuara and Kudo.[22]

We find different A-dependence for <n_> of $p + A \rightarrow \pi^-$ and $^{16}O + A \rightarrow \pi^-$ Eqs. (16) and (18), reflecting to some extent, different mechanisms of multiparticle production. These semi-empirical formulae, based on general grounds of kinematical considerations, may be useful to test various models proposed for the multiparticle production by nuclear reactions.

Acknowledgements

The authors wish to thank G. Gidal and I. Hinchliffe for many discussions and comments. One of the authors (TFH) renews acknowledgement to Prof. L. Leprince-Ringuet for having guided him with enduring inspiration to study *effet obus a balles* of reactions initiated by heavy nuclei of cosmic rays; he would like to thank L. Wagner for facilitating the work at LBL and the Tsi Jung Fund for the support.

References and Footnotes

1. P. Freier, E.J. Lofgren, E.P. Ney and F. Openheimer, Phys. Rev. 74, 1818 (1948) and A.L. Bradt and B. Peters, ibid., 75, 1779 (1949).
2. See e.g., J.D. Bjorken, Phys. Rev. D 27, 140 (1980).
3. Proc. XI Int. Conf. on Ultra Relativistic Nucleus-Nucleus Collisions—Quark matter 1987, North Holland Publishing Co., eds. H. Satz, et al., Z. Phys. C 38, No. 1/2 (1988).
4. See e.g., R. Hagedorn, Riv. Nuovo Cim. 6, No. 10 (1983).
5. NA5 Collaboration, C. de Marzo, et al., (a) Phys. Rev. D 26, 1019 (1982) and (b) ibid., 29, 2476 (1984).
6. N35 Collaboration, (a) H. Ströbele, et al., Z.P. C 38, 89 (1988) and (b) A. Bamberger, et al., Phys. Lett. B 205, 583 (1988).
7. WA 80 Collaboration, R. Albrecht, et al., (a) Phys. Lett., 202, 596 (1988) and (b) Z. Phys. C 38, 97 (1988).
8. T.T. Chou, Chen Ning Yang and E. Yen, Phys. Rev. Lett., 54, 510 (1985).
9. T.F. Hoang, (a) Partition temperature and fireball of handron-proton collision, Z. Phys. C. in press and (b) Partition temperature and asymmetric fireballs of π^+p and K^+p collisions.
10. BNL Exp. 802, reported by M.J. Tannenbaun in Proc. III Int. Conf. on Nucleus-Nucleus Collisions, St. Malo, France (1988), Nucl. Phys. A 488, 555^c (1988), Fig. 23.
11. T.F. Hoang, (a) Phys. Rev. D 12, 296 (1975) and (b) ibid., 38, 2729 (1988).
12. E. Fermi, Phys. Rev. 81, 683 (1951).

13. T.S. Li and K. Young, Phys. Rev. D 34, 142 (1987).

14. We have used the data in Fig. 23, of Ref. 10.

15. E116 Collaboration, D.S. Barton, et al., Phys. Rev. D 27, 2580 (1983). The Al and Ag data are left aside because some of the measurements are missing in their Table II.

16. (a) T.F. Hoang, Bruce Cork and H.J. Crawford, Z. Phys. C29, 611 (1985) and (b) T.F. Hoang and H.J. Crawford, ibid., 43, 219 (1989).

17. (a) L.P. Csernai, et al. Phys. Rev. D 29, 2669 (1989) and (9b) S. Daté, et al., ibid., 32, 619 (1985).

18. A.K. Abul-Magd, G. Alberi and L. Bertocchi, Phys. Lett., 30B, 182 (1969).

19. We have used the data of the following $p + A \rightarrow \pi^-$ experiments: (a) 9.9 GeV/c, M.A. Dasaeva, et al., Sov. J. Nucl. Phys. 39, 536 (1984); (b) 28 GeV/c, D.J. Miller, et al. Nuovo Cim. Lett, 13, 39 (1976); and (c) 360 GeV/c, J.L. Bailly, et al., Z. Phys. C 40, 215 (1988). For $<n_->_{pp}$, we use the data compiled in Ref. 16(b).

20. (a) EM07 Collaboration, H. von Gerstoff, et al., Phys. Rev. C 39, 1385 (1989) and (b) EM01 Collaboration, M.I. Admavich, et al., Phys. Rev. Lett., 62, 2801 (1989).

21. Note that T_p^* represents the average energy of a secondary π^- in the cms of the FB's of the projectile and the target (see Ref. 9a), T_p^* is related to T: $T_p^* = 3T + m_\pi$ so that it is practically constant, just like T as is listed in Tables I and II.

22. E.R. Nakamura and K. Kudo, Z. Phys. C. 40, 81 (1989).

Table I. Parameters of inclusive $p + A \rightarrow \pi^-$ at $P_{lab} = 200$ GeV/c, $\eta_{cm} = 3.02$, NA5 Collaboration, Ref. 5.

	pp	pAr	pXe
$\langle n- \rangle$	2.96±0.03	5.39±0.17	6.89±0.13
$\langle P_\perp \rangle$ (MeV/c)	366±2	376±3	363±3
η^*	≡0	0.44±0.03	0.50±0.01
T_p^* (GeV)	0.547±0.049	0.816±0.137	0.642±0.062

Table II. Parameters of inclusive $^{16}O + A \rightarrow h^\pm$ at 200 GeV/nucleon, $\eta_{cm} = 3.02$, WA80 Collision Ref. 7.

	Au	Ag	Cu	C
$\langle P_\perp \rangle$ (MeV/c)	~350	~350	~350	~350
η^*	0.44±0.05	0.25±0.02	0.13±0.02	–0.12±0.03
T_p^* (GeV)	0.831±0.076	0.764±0.099	0.498±0.024	0.870±0.086

Table IIIa. Comparison between experimental ratios $\langle n_- \rangle_{pA}/\langle n_- \rangle_{pp}$ and predictions by $R(A) = \frac{1}{2}(1 + A^{\alpha/3})$, Eq. (16) with $\alpha = 0.80$ according to NA5 data at $P_{lab} = 200$ GeV/c.

		Ratio $\langle n_- \rangle_{pA}/\langle n_- \rangle_{pp}$	
P_{lab} (GeV/c)	Target A	Experimental	Prediction
200	p	1.00	1.00
	^{40}Ar	1.83±0.08	1.80
	^{132}Xe	2.33±0.04	2.32
9.9	^{12}C	1.52±0.09	1.47
28	^{20}Ne	1.70±0.13	1.56
360	^{197}Au	2.76±0.10	2.56

Table IIIb. Comparison of the negative multiplicity of $^{16}O + A$ at 200 GeV/nucleon $R(A_1A_2) = \langle n- \rangle_{A_1A_2}/\langle n- \rangle_{pA_2}$ with the prediction Eq. (18), see text.

	Ratio $\langle n- \rangle_{A_1A_2}/\langle n- \rangle_{pA_2}$	
Target A_2	Experimental	Prediction
$^{15.7}O$	5.85±0.24	5.80
^{108}Ag	11.7±0.6	11.7
^{197}Au	15.4±0.5	15.2

O denotes the equivalent A of the mixture 20% He and 80% Ne of the steamer chamber.

Figure Captions

Fig. 1. Pseudo-rapidity distributions of inclusive $p + A \rightarrow \pi^-$ at $P_{lab} = 220$ GeV/c. The peak shift, η^*, with respect to the cms is characteristic of the asymmetry of the projectile and the target fireballs. The curves are partition temperature T_p model fits. Parameters are in Table I. The shift parameters η^* are shown by the dot-dash lines.

Fig. 2. Pseudo-rapidity distributions of $A_1 + A_2 \rightarrow h^{\pm}$ at 200 GeV/A. WA 80 experiment, Ref. 7. Note the increase of the peak shift η^* with A. The curves represent the T_p model its. Parameters are listed in Table II.

Fig. 3. Behaviour of the peak-shift parameter η^*. The values of η^* for pA (full circles) and $A_1 + A_2$ (open circles) reactions in Tables I and II are plotted vs. the difference in nuclear size. The straight line is the least-squares fit to these two sets of data. The crosses, not included in the fit, are from a BNL experiment at 14.5 GeV/A, Ref. 10, indicating energy-independence of η^*.

Fig. 4. Plots of η-distributions (in percentage) vs. $\eta - \eta^*$ The curve shows the property required by the Chou-Yang-Yen formula, Eq. (5), see text.

Fig. 5. Energy-loss of the projectile fireball (FB) passing through a nuclear target, $p + A \rightarrow \pi^- + ...$ at 100 GeV/c. Data from the MIT-Fermilab experiment, Ref. 15. The plot represents the Lorentz factor of the FB vs. the effective nuclear radius of the target, see text. The curve represents an exponential fit with a mfp $\ell = 6.21 \pm 0.03$ fm.

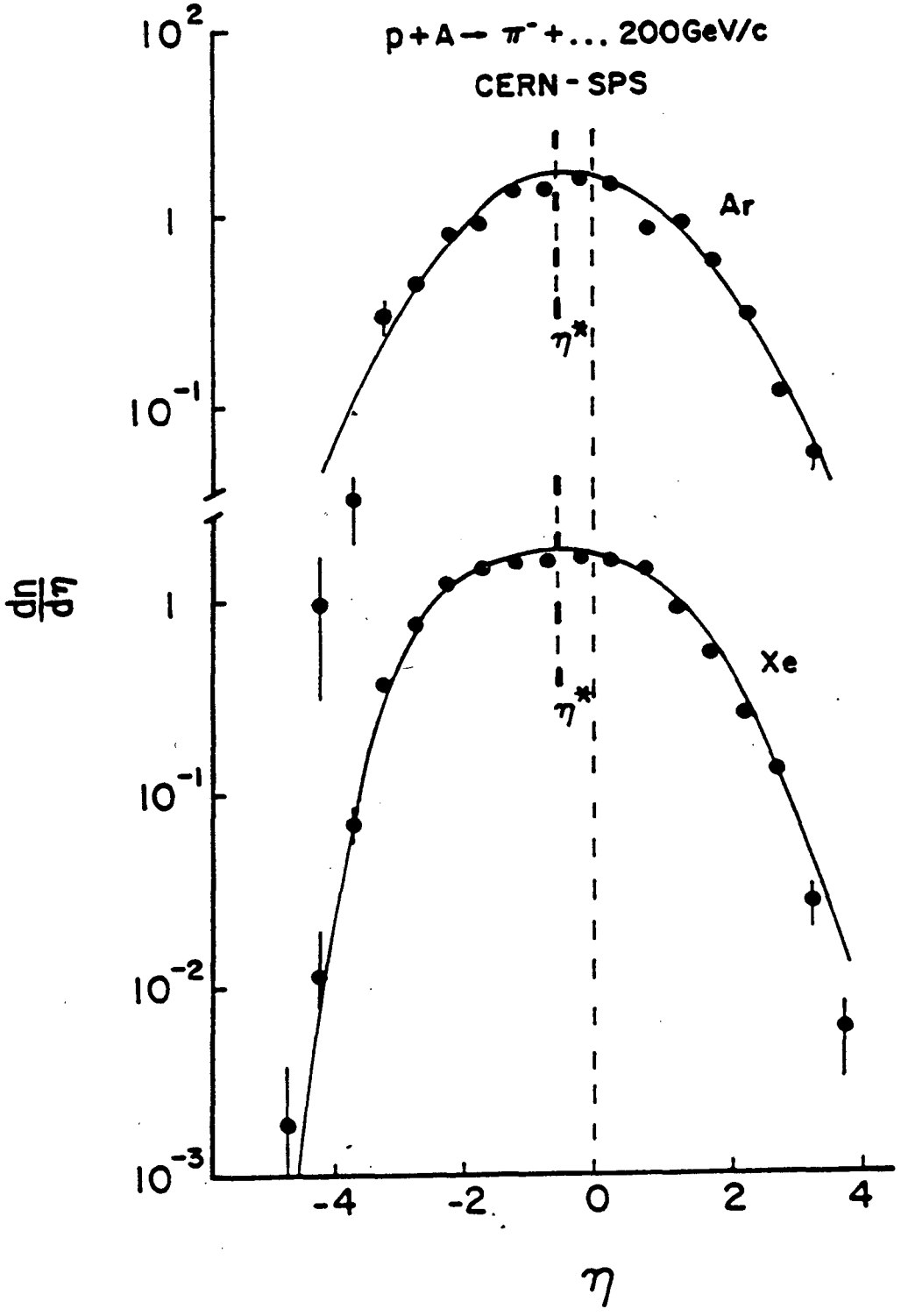
p+A→ π⁻+... 200GeV/c
CERN - SPS
Ar
Xe
η*
η*
dn/dη
η
10²
1
10⁻¹
10⁻²
10⁻³
-4
-2
0
2
4
XBL 898-3127

Fig. 1

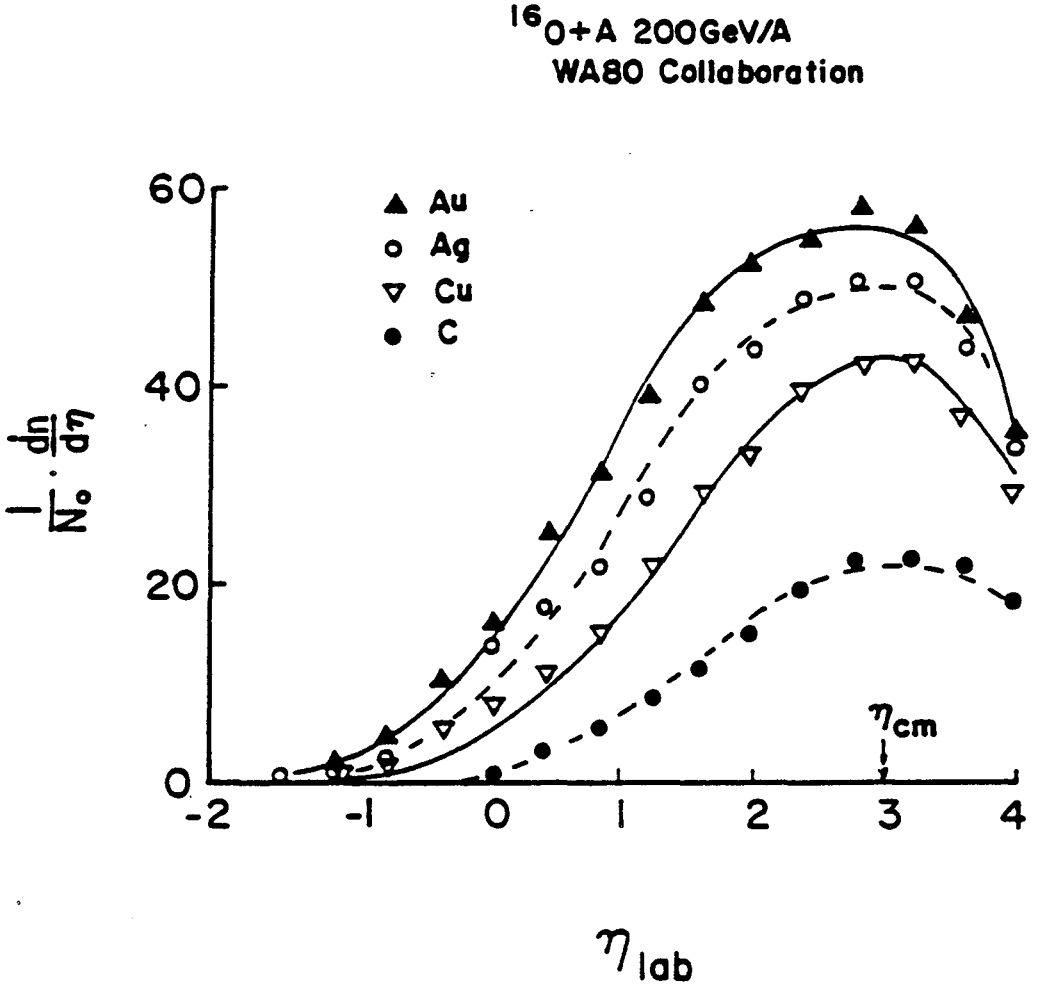
^{16}O+A 200GeV/A
WA80 Collaboration
Au
Ag
Cu
C
60
40
20
0
-2
-1
0
1
2
3
4
η_{cm}
$\frac{1}{N^\circ}\frac{dN}{d\eta}$
η_{lab}
XBL 898-3128

Fig 2

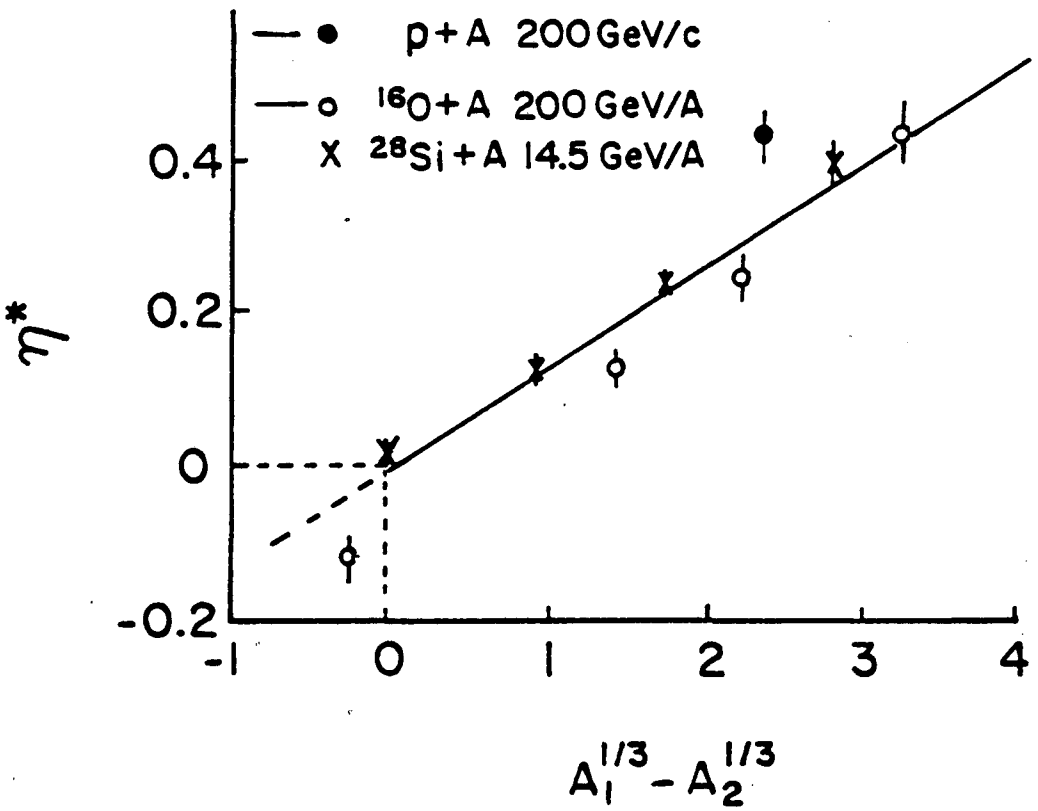

XBL 898-3130

Fig. 3

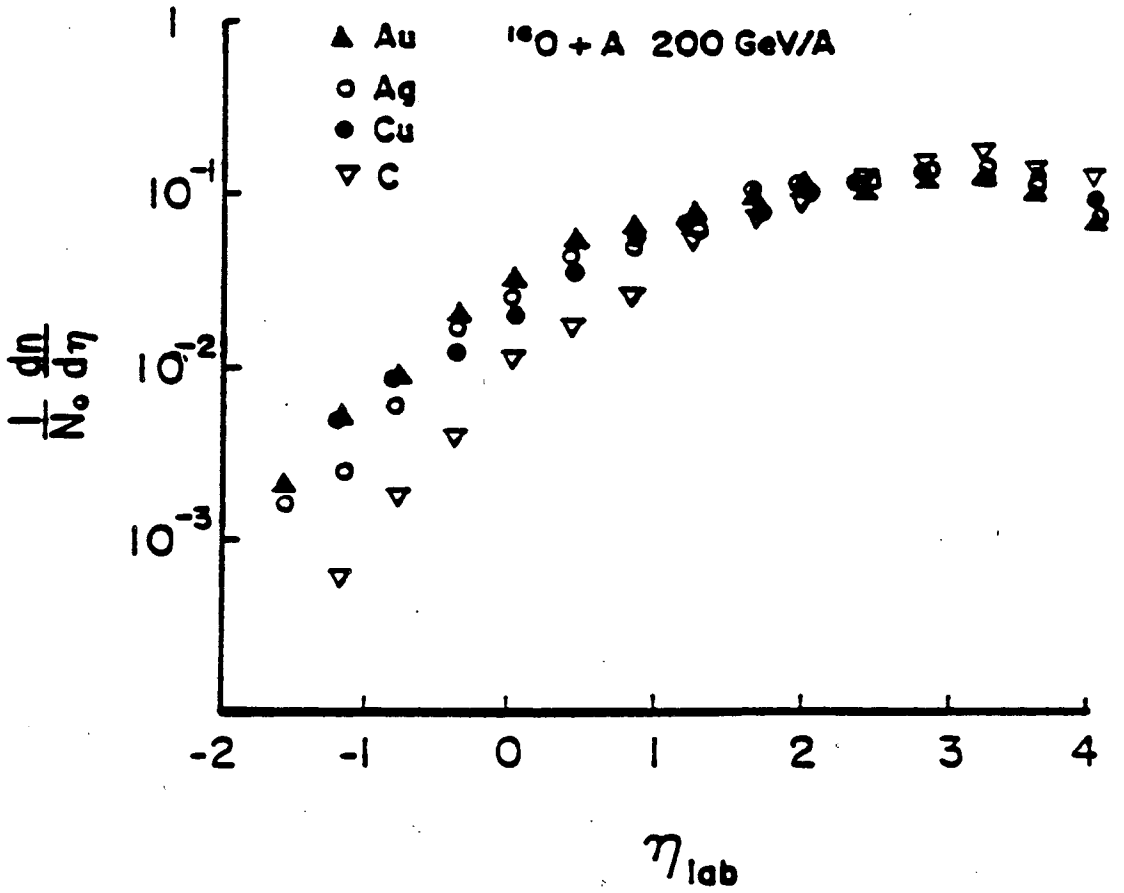
Au
Ag
Cu
C
$^{16}O + A$ 200 GeV/A
1
10^{-1}
10^{-2}
10^{-3}
$\frac{1}{N_0}\frac{dn}{d\eta}$
-2
-1
0
1
2
3
4
η_{lab}

Fig. 4

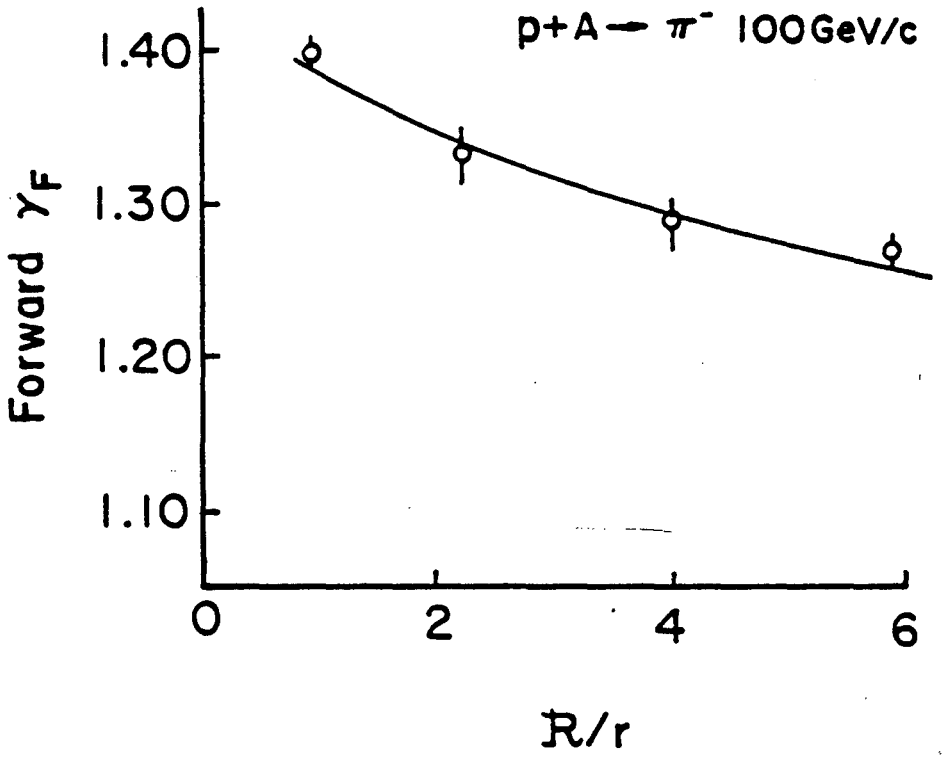

XBL 898-3129

Fig. 5

LAWRENCE BERKELEY LABORATORY
TECHNICAL INFORMATION DEPARTMENT
1 CYCLOTRON ROAD
BERKELEY, CALIFORNIA 94720